OPEN ACCESS

Saudi Journal of Engineering and Technology
Abbreviated Key Title: Saudi J Eng Technol
ISSN 2415-6272 (Print) | ISSN 2415-6264 (Online)
Scholars Middle East Publishers, Dubai, United Arab Emirates
Journal homepage: https://saudijournals.com

Original Research Article

Vibration Analysis of Uniform Flexible Beams under Large Deformation with Uniformly Continuous Mass Elements Using the Equivalent Pseudolinear System

Onodagu, P. D[1*], Uzodinma, F. C[1], Aginam, H. C[1]

[1]Department of Civil Engineering, Nnamdi Azikiwe University, Awka, Nigeria

DOI: 10.36348/sjet.2024.v09i05.001 | **Received:** 23.03.2024 | **Accepted:** 29.04.2024 | **Published:** 06.05.2024

***Corresponding author:** Onodagu, P. D
Department of Civil Engineering, Nnamdi Azikiwe University, Awka, Nigeria

Abstract

This paper analyses vibration of uniform flexible simply supported rectangular isotropic beam under large deformation with uniformly distributed mass elements. The method of equivalent pseudolinear systems was employed. The deformation of the beam was assumed to be large and the beam was also assumed to be inextensible. The expressions for elastic and nonlinear bending moments were determined. The numerical values of horizontal displacements of the movable support, and the equivalent lengths at various depth-to-breadth (aspect) ratios were determined. The corresponding equivalent pseudolinear systems for various nonlinear bending moment diagrams at various aspect ratios were determined. Consequently the concentrated loads yielding the equivalent pseudolinear systems were converted to point masses using the gravitational acceleration; and subsequently a unit load system was applied successively and independently at each mass point. The Vereshchagin's method was applied to determine the displacements for canonical equations of motion. Non-trivial solution of the canonical equations at each aspect ratio was sought for the desired eigenvalues. The first mode frequencies at aspect ratios, $\beta = 1.00$ and $\beta = 1.25$ are complex eigenvalues. Also the natural frequencies exhibit hard-spring type with aspect ratios; and the fundamental frequencies for all the aspect ratios are at seventh mode. Conclusively, the dynamic stability of the flexible rectangular beam of 0.25m-breadth and 15m-undeformed length is not guaranteed when the aspect ratio is less than or equal to 1.25. It is also concluded that deepness of the flexible rectangular beam loaded with uniformly distributed mass elements influences the vibratory characteristics.

Keywords: Vibration, Large Deformation, Equivalent Pseudolinear, Simply Supported, Flexible Beam, Continuous Mass Element, Canonical Equations, Aspect Ratio, Complex Eigenvalue, Fundamental Frequency.

1.0 INTRODUCTION

The vibrational behaviour and large deformation characteristics associated with flexible beams have been imposing a lot of challenges in the applications of flexible beam structures. Sequel to their extremely vibratory and large deformation characteristics, a lot of research works has been done to find solutions to the problems of flexible beams. The earliest research works on the analysis of flexible beams were carried out in the span of 18th century to the middle of 19th century by the Bernoulli family: Jacob, Johann and Daniel, and later by L. Euler, J. L. Lagrange and G.A.A Plana (Fertis, 1999). In their works, they sought the solution of various problems of elastica by using the relation between the curvature and the bending moment.

However, with the advances in science of materials and technological innovations in industries, there have been increases in environmental and industrial demands on the applications of flexible beam structures. Flexible beam structures have been used as structural systems in areas such as marine riser system, aircraft wings, flexible manipulator system, flapping wing of robotic aircraft, fire rescue turntable ladder system, truss structures, space telescopes and space stations, etc. (He and Liu, 2019; Pai and Palazotto, 1996). It is very important to recognize that a beam can be classified as a flexible beam if the length of the beam is extremely very large when compared to the other two dimensions of the beam.

Consequent upon these various applications, many research works have been done on the analysis and design of flexible beam structures; and furthermore, a lot of research works has been done on the methods for vibration control of flexible structures.

Weeks and Jackson (1971) investigated on the vibration characteristics of flexible cantilever beam under a nonlinear deformed equilibrium state by using the perturbation method.

Fertis and Afonta (1992), Fertis and Lee (1991), Fertis, Taneja and Lee (1991), Fertis and Afonta (1993) and Fertis and Schubert (1994) generally employed the method of equivalent system to either solve vibrational problem of undamped variable stiffness flexible bars or to carry out inelastic analysis of prismatic and nonprismatic structural members of flexible characteristics. Modal analysis of a flexible beam attached with multiple absorbers was carried out (Li *et al.*, 2012). Also, large-deformation analysis of flexible beam was investigated by Pai and Palazotto (1996) and Kwark (1998) analysed the dynamics of slewing flexible beams by modeling new admissible functions based on discretization process. Chen and Levy (1999) used smart damping structures to carry out vibration analysis and vibration control of flexible beam with the intention to determine the effects of temperature on frequency and loss factor for the structure.

Furthermore, into the 21st century, a quite lot of research works has been unabatedly done on flexible beam structures. Nayfeh *et al*., (2003) investigated the free vibrations of flexible beams undergoing overall motions in two dimensions by using the Euler-Bernoulli beam theory. Also, Shvartsman (2009) investigated on the responses of flexible cantilever beam subjected to two follower forces under static large deflection problem. Nonlinear dynamic analysis of the Timoshenko flexible beams using the continuous wavelet transform and the traditional Fourier transform methods was carried out (Awrejcewicz *et al*., 2012).

Gafsi *et al*., (2014) investigated on the effect of confinement of vibrations for variable-geometry nonlinear flexible beam. Trivedi *et al*., (2016) employed Hamiltonian modeling to analyse the buckling behaviour of a nonlinear Euler-Bernoulli flexible beam with actuation at the bottom. Jianshu *et al*., (2017) employed the sub-structuring technique for dynamic analysis of flexible beams with large deformation. Further research works include Zhang and Vang (2020) and Guo *et al*., (2020) who studied the vibration of flexible beam with interior fluid and the dynamic analysis of the flexible hub-beam system based on rigid-flexible coupling mechanism respectively. Fan and Zhu (2016) worked on the accuracy of singularity-free formulation of a three dimensional curved Euler-Bernoulli beam with large deformations and large rotations for flexible multibody dynamic analysis.

From the review of the previous research works on flexible beam structures, it is certain that there exists no close-form solution to determine the exact behaviour of nonlinear flexible beam structures. Therefore, this paper proposes to employ very simple and straight forward methods to determine the vibrational frequencies of large deformation of simply supported flexible rectangular isotropic beam, which are closely approximating the exact solutions to nonlinear flexible beam problems. This proposition is to be achieved by using these set down objectives: First is to utilize the Fertis equivalent pseudolinear system to linearize the nonlinear responses of flexible beams with simply supported boundary conditions. Secondly, this paper is to employ the Mohr-Vereshchagin's methods to determine the canonical equations of motion (Darkov, 1983). Thirdly, it determines the associated vibrational natural frequencies.

2.0 ANALYTICAL FORMATION

In this paper, the vibrational responses of uniform flexible beam with simply supported boundary conditions under large deformations, and subjected to uniformly distributed mass elements will be studied. The analytical models to be employed are the Fertis pseudolinear equivalent system model (Fertis, 1999); and the Mohr-Vereshchagin's methods (Darkov, 1983).

2.1 Derivation of Pseudolinear Equivalent Systems

The pseudolinear equivalent system model was developed by D.G. Fertis (Fertis, 1999). This model tends to solve large deflection of nonlinear problem by utilizing an equivalent pseudolinear system, which has an identical deflection curve as the initial nonlinear problem. In the process, the initial nonlinear problem is transformed into a pseudolinear equivalent system, which will have uniform stiffness EI throughout its equivalent length, and which may be loaded differently from the original nonlinear system and this can be solved by applying linear analysis.

The derivation of pseudolinear equivalent system can be developed by employing the Euler-Bernoulli law, which states that if the deflection of the beam is not small, the slope of the deflection can never be neglected in the expression describing the curvature. Also, the law states that the bending moment M is proportional to the change in the curvature developed as a result of the action of the externally applied load (Fertis, 1999). Thus, this can be mathematically stated as given in Eqn. (2.1).

$$\frac{1}{r} = \frac{d\emptyset}{dx_a} = \frac{-M_x}{E_x I_x} \qquad (2.1)$$

Where r is the radius of curvature, $\emptyset$ is the slope at any given point x_a along the arc length of the bending beam, E_x is the modulus of elasticity which may be varied along the length of the beam, I_x is the cross-

sectional moment of inertia which may also be varied along the length of the beam, and M_x is the bending moment at any given point x along the length of the beam.

In the derivation, it is fundamentally assumed that the beam structural system is inextensible so that the arc length of the deflection curve is equal to the initial length of the beam structure.

In this paper, the rectangular coordinate system of x and y is adopted so that Eqn. (2.1) can be expressed as given in Eqn. (2.2).

$$\frac{y''}{[1+(y')^2]^{3/2}} = \frac{-M_x}{E_x I_x} \tag{2.2}$$

Where,

$$y'' = \frac{d^2y}{dx^2} \text{ and } y' = \frac{dy}{dx} \tag{2.3}$$

Eqn. (2.2) is a second order nonlinear equation in which its exact solution yields the true shape of the deflection configuration (elastica) of a flexible member.

Let the variable stiffness E_xI_x be defined by the expression as given in Eqn. (2.4).

$$E_x I_x = E_1 I_1 u(x) v(x) \tag{2.4}$$

Where u(x) represents the variation of E_x with respect to fixed value E_1 and v(x) represents the variation of I_x with respect to fixed value I_1.

Consequently, Eqn. (2.2) can be written as given by Eqn. (2.5).

$$\frac{y''}{[1+(y')^2]^{3/2}} = \frac{-1}{E_1 I_1} . \frac{M_x}{u(x)v(x)} \tag{2.5}$$

By integrating Eqn. (2.5) twice with respect to x, yields the transverse displacement y(x) as expressed in Eqn. (2.6) (Fertis, 1999).

$$y(x) = \frac{1}{E_1 I_1} \int \left\{ - \int [1+(y')^2]^{3/2} \frac{M_x dx}{u(x)v(x)} \right\} dx + C_1 \int dx + C_2 \tag{2.6}$$

Where C_1 and C_2 are undetermined constants of integration, which can be determined by using the boundary conditions. Let there be a structural beam element with constant stiffness E_1I_1 which has length and reference axes that are of identical with the one in Eqn.(2.6); then the expression for its large deflection y_e is as given by Eqn. (2.7).

$$y_e = \frac{1}{E_1 I_1} \int \left\{ - \int [1+(y')^2]^{3/2} M_e dx \right\} dx + K_1 \int dx + K_2 \tag{2.7}$$

Where M_e is the bending moment at any given cross-section x, and K_1 and K_2 are the undetermined constants of integration. Thus if y and y_e as given in Eqns. (2.6) and (2.7) respectively are identical, then it implies that $C_1 = K_1$ and $C_2 = K_2$ so that:

$$\int \left\{ - \int [1+(y')^2]^{3/2} \frac{M_x dx}{u(x)v(x)} \right\} dx = \int \left\{ - \int [1+(y')^2]^{3/2} M_e dx \right\} dx \tag{2.8}$$

Therefore given the conditions which specify that $C_1 = K_1$ and $C_2 = K_2$ are to be satisfied, then it implies that these conditions are absolutely satisfied only and only if the two beam structural elements have the same length and boundary conditions; and these condition are particularly satisfied if $y_e' = y'$. Thus it can be written that:

$$M_e = \frac{M_x}{u(x)v(x)} \tag{2.9}$$

From Eqn. (2.8), it can be stated that:

$$[1+(y')^2]^{3/2}M_e = [1+(y')^2]^{3/2}\frac{M_x}{u(x)v(x)} \qquad (2.10)$$

Therefore, for the analysis of large deflections and rotations, where $(y')^2$ and $(y'_e)^2$ cannot be neglected, then Eqn. (2.10) suggests that the moment M'_e of equivalent pseudolinear system of constant E_1I_1 can be evaluated from the expression as stated in Eqn.(2.11) (Fertis, 1999).

$$M'_e = [1+(y')^2]^{3/2}\cdot\frac{M_x}{u(x)v(x)} = Z_e\cdot\frac{M_x}{u(x)v(x)} \qquad (2.11)$$

Where $Z_e = [1+(y')^2]^{3/2}$ (2.12)

From Eqn. (2.5), it is deduced that the differential equation representing the pseudolinear equivalent system of constant stiffness E_1I_1 is as given by Eqn. (2.13).

$$y'' = \frac{M'_e}{E_1I_1} \qquad (2.13)$$

Upon the determination of M'_e, which is the product of elastic bending moment M_x and $[1+(y')^2]^{3/2}$ divided by the stiffness variations $u(x)v(x)$ then the transformation that yields the pseudolinear equivalent system of constant stiffness E_1I_1, with its characteristic loading is evaluated.

In this paper, the concentrated loads and the associated loading points as obtained in the pseudolinear equivalent system will be transformed into point masses and mass locations respectively, and those masses will be used in the evaluation of vibrational frequencies by using the Mohr-Vereshchagin's methods (Darkov, 1983)

2.2 Application to Simply Supported Flexible Beam

Fig. 1 shows an elastic isotopic homogeneous simple supported flexible beam of rectangular cross-section with the characteristic dimensions defined as follows: L is the length, b is the breadth and h is the thickness. The beam parameters are invariant in young modulus E and mass density ρ.

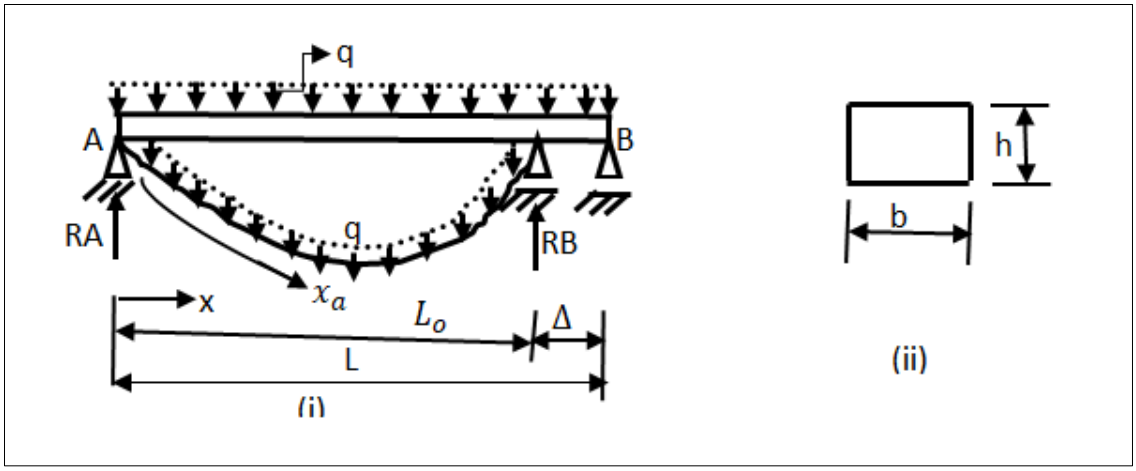

Fig. 1 (i) simply supported flexible beam loaded with uniformly distributed mass element; and showing the deflected configuration

(ii) Shows the cross-section of the beam

From Fig. 1 (ii), the expression for moment of inertia is given as in Eqn. (2.14).

$$I = \frac{bh^3}{12} \qquad (2.14)$$

Let $\beta = {}^{h}/_{b}$ or $h = \beta b$ (2.15)

Where β is the beam depth-to-breadth (aspect) ratio.

By substituting for h from Eqn. (2.15) into Eqn. (2.14) yields Eqn. (2.16)

$$I = \frac{b^4\beta^3}{12} \qquad (2.16)$$

From Fig. 1 (i), the bending moment M_x at any point in the interval $0 \leq x \leq L_o$ is given as expressed in Eqn. (2.17)

$$M_x = \frac{qLx}{2} - \frac{qxx_a}{2} \qquad (2.17)$$

Where the expression for x_a is defined as given in Eqn. (2.18) (Fertis, 1999).

$$x_a = \int_0^x \sqrt{1 + (y')^2}\, dx \qquad (2.18)$$

By substituting for x_a in Eqn. (2.17) yields:

$$M_x = \frac{qLx}{2} - \frac{qx}{2}\int_0^x \sqrt{1 + (y')^2}\, dx \qquad (2.19)$$

Furthermore, by substituting Eqn. (2.19) into Euler-Bernoulli equation of Eqn. (2.2) yields:

$$\frac{y''}{[1 + (y')^2]^{3/2}} = \frac{qx}{2EI}\left\{-L + \int_0^x \sqrt{1 + (y')^2}\, dx\right\} \qquad (2.20)$$

Eqn. (2.20) is an expression that defines the exact nonlinear differential equation for the flexible beam problem. The close-form solution to Eqn. (2.20) is difficult; but a very high approximation to the solution of Eqn. (2.20) can be achieved by assuming that x_a is a function of horizontal displacement of the movable edge of the beam, and it is defined as given in Eqn. (2.21) (Fertis, 1999).

$$x_a = x + \Delta(x) \qquad (2.21)$$

Where Δ(x) may be a variation in x-quantity. Suppose Δ(x) is constant so that Δ(x) = Δ, then Eqn.(2.21) becomes Eqn. (2.22).

$$x_a = x + \Delta \qquad (2.22)$$

By substituting Eqn. (2.22) into Eqn. (2.17) yields:

$$M_x = \frac{qLx}{2} - \frac{qx}{2}(x + \Delta) = \frac{qx}{2}(L - \Delta) - \frac{qx^2}{2} \qquad (2.23)$$

By substituting Eqn.(2.23) into the Euler-Bernoulli equation of Eqn. (2.2), yields Eqn. (2.24).

$$\frac{y''}{[1 + (y')^2]^{3/2}} = \frac{q}{2EI}[x^2 - (L - \Delta)x] \qquad (2.24)$$

Let

$$\lambda(x) = \frac{y''}{[1 + (y')^2]^{3/2}} \qquad (2.25)$$

Then Eqn. (2.24) can be written as:

$$\lambda(x) = \frac{q}{2EI}[x^2 - (L - \Delta)x] \qquad (2.26)$$

By integrating Eqn. (2.26) once with respect to x yields Eqn. (2.27).

$$\int \lambda(x)dx = \frac{q}{12EI}[2x^3 - 3(L - \Delta)x^2] + C \qquad (2.27)$$

Or

$$\frac{y'}{\sqrt{1+(y')^2}} = \frac{q}{12EI}[2x^3 - 3(L-\Delta)x^2] + C \qquad (2.27a)$$

Where C is the constant of integration, which can be determined from the boundary condition that the slope, y' is zero at ${}^{L_o}/_{2}$ where $L_o = L - \Delta$ (2.28)

From the boundary condition that $y' = 0$ at $x = {}^{L_o}/_{2}$' then:

$$C = \frac{q}{12EI}\left[\frac{(L-\Delta)^3}{2}\right] \quad (2.29)$$

Thus Eqn. (2.27a) can be written as in Eqn. (2.30).

$$\frac{y'}{\sqrt{1+(y')^2}} = \frac{q}{24EI}[4x^3 - 6(L-\Delta)x^2 + (L-\Delta)^3] \qquad (2.30)$$

By solving Eqn. (2.30) with respect to y' yields Eqn. (2.31).

$$y'(x) = \frac{G(x)}{\sqrt{1-[G(x)]^2}} \qquad (2.31)$$

Where

$$G(x) = \frac{q}{24EI}[4x^3 - 6(L-\Delta)x^2 + (L-\Delta)^3] \qquad (2.32)$$

Or by invoking Eqn. (2.16), then Eqn. (2.32) becomes:

$$G(x) = \frac{q}{2Eb^4\beta^3}[4x^3 - 6(L-\Delta)x^2 + (L-\Delta)^3] \qquad (2.33)$$

Here the unknown quantity to be determined is Δ, and it can be determined by selecting Δ in a trial and error process, which will satisfy the expression given in Eqn. (2.34).

$$L = \int_0^{L_o} \sqrt{1+(y')^2}\,dx \qquad (2.34)$$

Where L is the initial undeformed length and L_o is as defined in Eqn. (2.28).

Upon the determination of the exact value of Δ, then the value of M_e' of Eqn. (2.11) is determined at various points of x-values.

2.3 RESULTS

In this work, the investigation was carried out at various aspect ratios of beam thickness to beam breadth, $\left(\beta = \frac{h}{b}\right)$, ranging from 1 to 2 at a step size of 0.25, and the value of Δ for each aspect ratio was determined and consequently the values of elastic bending moments, M_x and equivalent nonlinear bending moments, M_e' were determined. Tables 2.1, 2.2, 2.3, 2.4 and 2.5 show the values for M_x and M_e' at aspect ratios 1, 1.25, 1.50, 1.75 and 2.0 respectively for selected x-point values in the interval of $0 \leq x \leq L_0$. The equivalent nonlinear bending moment diagrams and the associated equivalent pseudolinear systems for the corresponding aspect ratios are shown in Figures 2.1, 2.2, 2.3, 2.4 and 2.5 respectively. However, the values of M_e' at these selected x-points were plotted in juxtaposition with the equivalent nonlinear bending moment diagrams, from which the equivalent pseudolinear systems could be determined.

Table 2.1: The values of bending moments for aspect ratio β = 1

L = 15m; Δ = 0.3375m; L_o = 14.6625m		
x	M_x (* 10^6)	M_e' (* 10^6)
0	0	0
2.095	1.31645	1.47057

4.399	2.25746	2.35945
5.865	2.57987	2.61068
7.331	2.68736	2.68736
8.798	2.57979	2.61063
10.473	2.19383	2.30627
12.568	1.31618	1.4703
14.6625	0	0

Table 2.2: The values of bending moments for aspect ratio β = 1.25

L = 15m; Δ = 0.0954m; L_o = 14.9046m		
x	M_x (* 10^6)	$M_e^{'}$ (* 10^6)
0	0	0
2.129	1.35996	1.40305
4.258	2.26666	2.29929
5.962	2.66579	2.67493

Table 2.2: The values of bending moments for aspect ratio β = 1.25, cont'd

L = 15m; Δ = 0.0954m; L_o = 14.9046m		
7.453	2.77684	2.77684
8.942	2.66588	2.67501
10.646	2.26685	2.29947
12.775	1.36028	1.40338
14.9046	0	0

Table 2.3: The values of bending moments for aspect ratio β = 1.50

L = 15m; Δ = 0.02966m; L_o = 14.97034m		
x	M_x (* 10^6)	$M_e^{'}$ (* 10^6)
0	0	0
2.139	1.37231	1.38701
4.277	2.28677	2.298
5.988	2.68931	2.69248
7.485	2.80139	2.80139
8.982	2.68936	2.69253
10.693	2.28688	2.29811
12.832	1.37196	1.38665
14.97034	0	0

Table 2.4: The values of bending moments for aspect ratio β = 1.75

L = 15m; Δ = 0.01296m; L_o = 14.98704m		
x	M_x (* 10^6)	$M_e^{'}$ (* 10^6)
0	0	0
2.142	1.3757	1.38155
4.284	2.29259	2.29707
5.995	2.69536	2.69663
7.494	2.80764	2.80764
8.992	2.69537	2.69664

Table 2.4: The values of bending moments for aspect ratio β = 1.75, cont'd

L = 15m; Δ = 0.01296m; L_o = 14.98704m		
10.703	2.2926	2.29708
12.845	1.375573	1.38157
14.98704	0	0

Table 2 5: The values of bending moments for aspect ratio β = 2.0

L = 15m; Δ = 0.00567m; L_o = 14.99433m		
x	M_x (* 10^6)	$M_e^{'}$ (* 10^6)
0	0	0
2.142	1.37648	1.37911

4.284	2.29415	2.29617
5.998	2.698	2.69857
7.497	2.81037	2.81037
8.997	2.6979	2.69847
10.710	2.29426	2.29628
12.852	1.37666	1.37929
14.99433	0	0

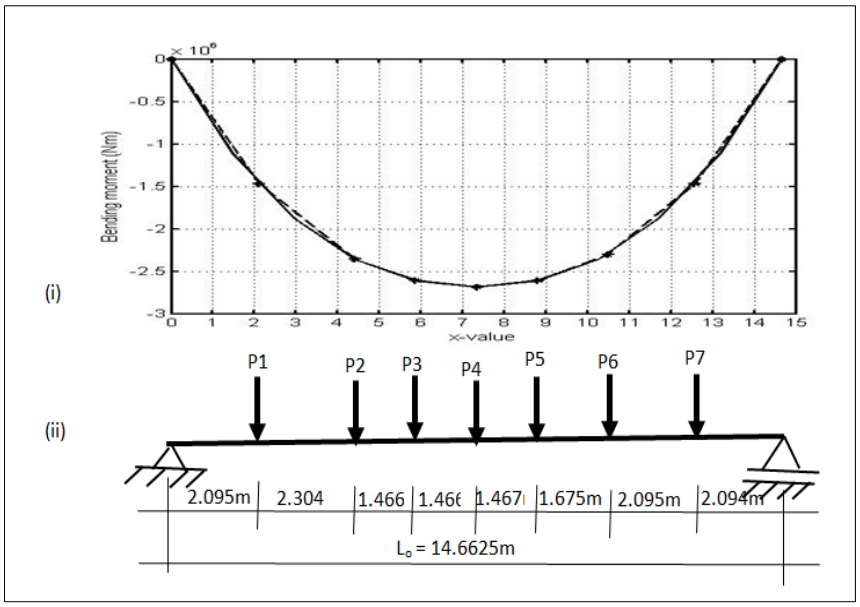

Fig. 2.1 (i): The nonlinear bending moment diagram for β = 1.0
Fig. 2.1 (ii): The corresponding equivalent pseudolinear system for the beam.

Key to Fig. 2.1
P1 = 316165.8111N; P2 = 214358.083N; P3 = 119126.8758N; P4 = 104411.9236N;
P5 = 129748.6840N; P6 = 217162.3696N; P7 = 302950.3535N

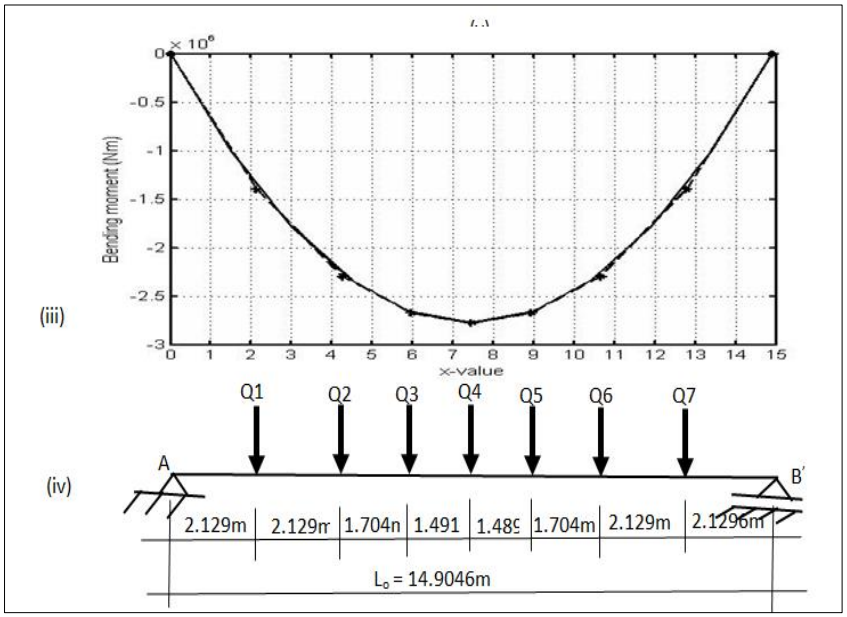

Fig. 2.2 (iii): The nonlinear bending moment for β = 1.25
Fig. 2.2 (iv): The corresponding equivalent pseudolinear system for the beam.

Key to Fig. 2.2
Q1 = 238060.1222N; Q2 = 200506.3184N; Q3 = 152108.4842N; Q4 = 136726.5737N;
Q5 = 152005.0125N; Q6 = 200508.6393N; Q7 = 238082.4607N

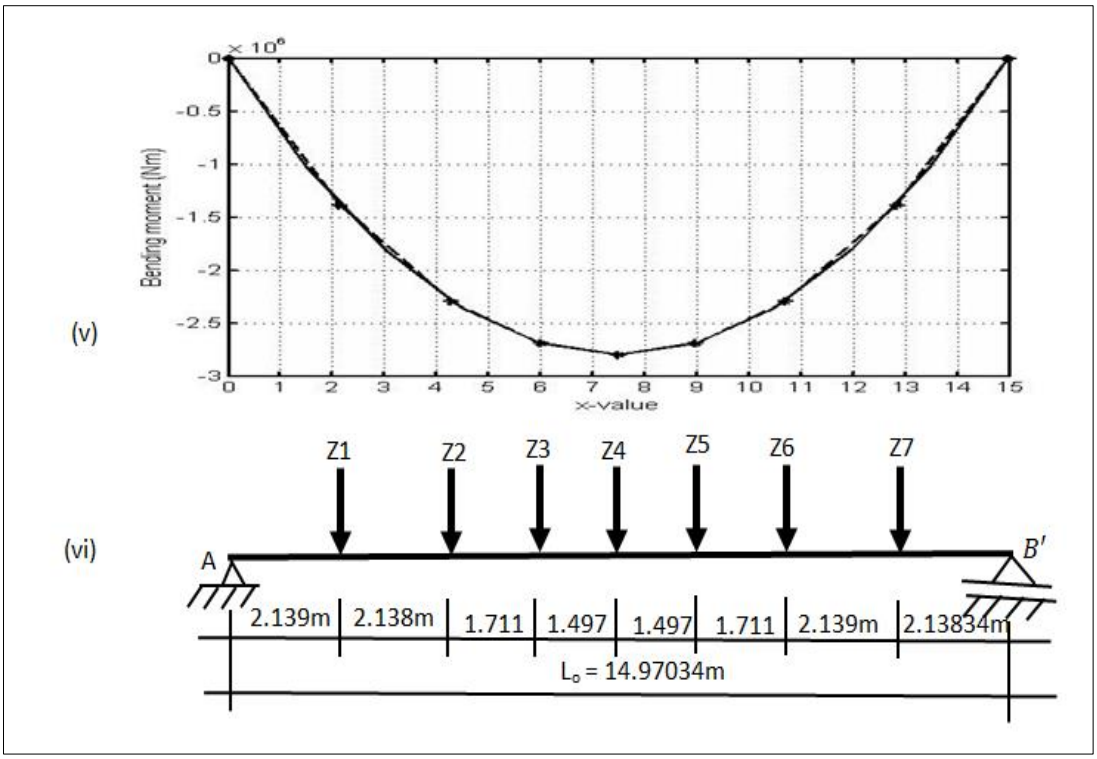

Fig. 2.3 (v): The nonlinear bending moment diagram for β = 1.50
Fig. 2.3 (vi): The corresponding Equivalent Pseudolinear system for the beam element

Key to Fig. 2.3

Z1 = 222344.0419N; Z2 = 195539.2499N; Z3 = 157803.0599N; Z4 = 145470.9419N;
Z5 = 157801.3927N; Z6 = 195594.8434N; Z7 = 222355.3017N

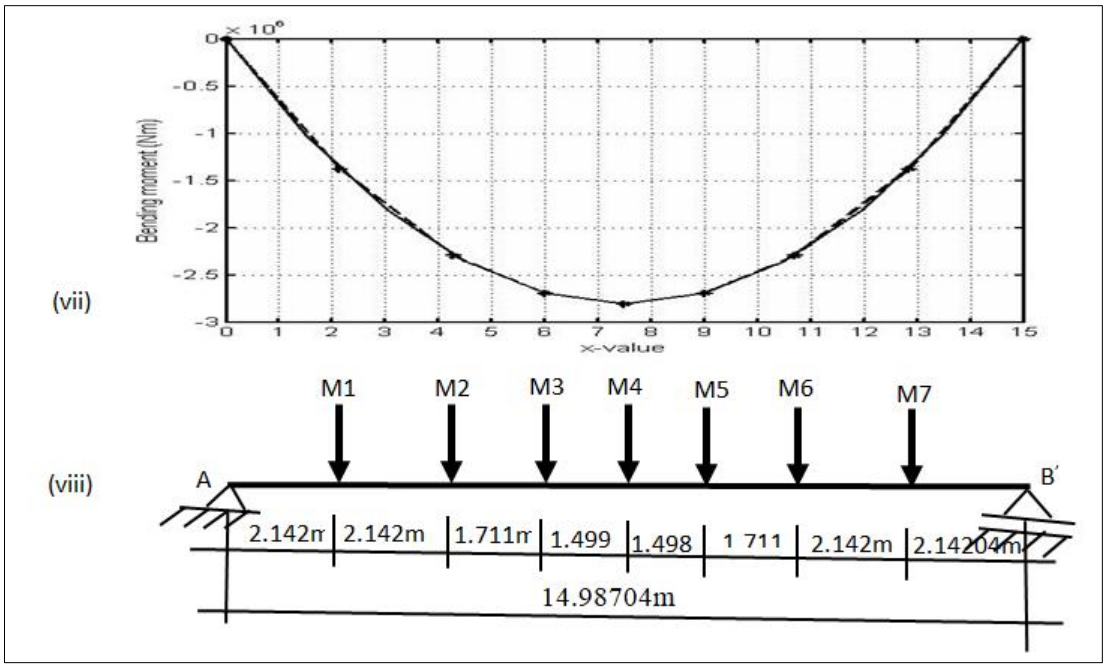

Fig. 2.4 (vii): The nonlinear bending moment diagram for β = 1.75
Fig. 2.4 (viii): The corresponding Equivalent Pseudolinear system for the beam

Key to Fig. 2.4

M1 = 217567.6938N; M2 = 193889.3773N; M3 = 159468.2174N; M3 = 159468.2174N;
M4 = 148154.8358N; M5 = 159425.4564N; M6 = 193884.7088N; M7 = 217569.6549N

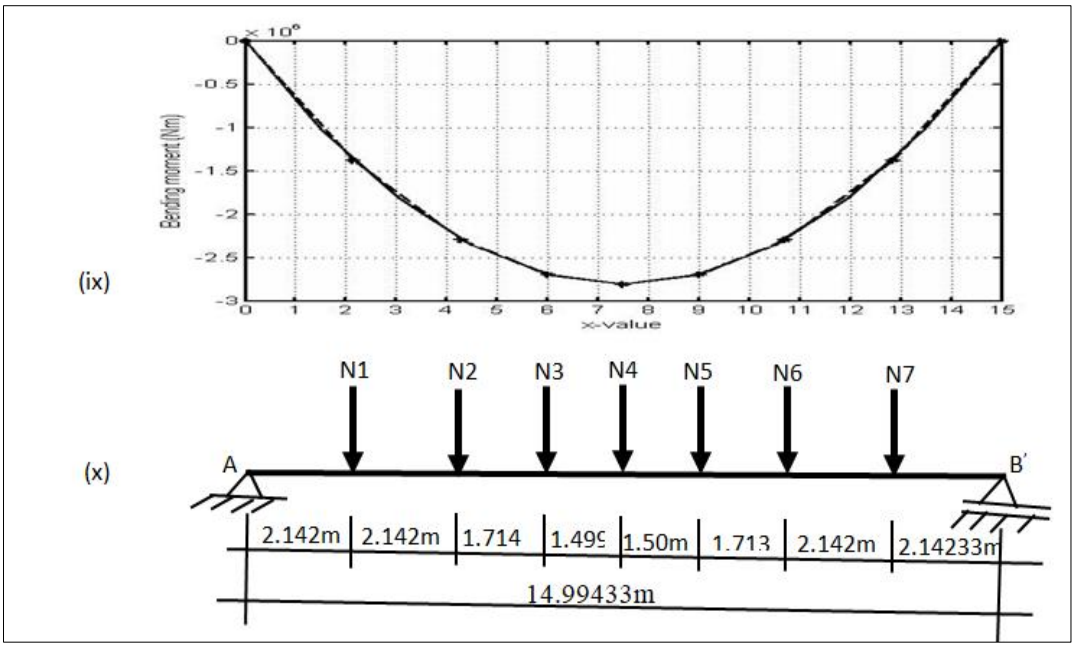

Fig. 2.5 (ix): The nonlinear bending moment diagram for β = 2.0
Fig. 2.5 (x): The corresponding equivalent pseudolinear system for the beam.

Key to Fig. 2.5
N1 = 215709.6171N; N2 = 193360.1243N; N3 = 160189.4067N; N4 = 149183.0554N;
N5 = 160186.9235N; N6 = 193312.9831N; N7 = 215727.1415N

2.3.1 The Equivalent Pseudolinear System

The equivalent pseudolinear system was determined by joining the selected points on the nonlinear bending moment diagram with straight cords (lines) and then the method of statics was employed to determine the concentrated loads. These points on the nonlinear bending moment diagram have to be adjusted to give a system of concentrated loads that would yield equivalent stresses to that of initially applied loads on the equivalent length of the flexible beam element.

2.3.2 Determination of the Vibration Frequencies

In this work, the determination of the vibration frequencies of uniform flexible beams subjected to continuous mass element are approximated by considering the concentrated loads on the equivalent lengths of the beams as point mass system. These concentrated loads were transformed into point masses by dividing the concentrated load with the value of gravitational acceleration ($9.81ms^{-2}$). On the successful transformation of the concentrated loads to mass system, a unit load system was applied successively and independently at mass point and the respective resulting bending moment diagram was drawn as shown in Appendix A. And in accordance with the Mohr-Vereshchagin's methods, these stress diagrams were multiplied by one another to yield the displacements for canonical equations of motions. Hence the nontrivial solution of the canonical equations yields the desired vibration frequencies. Table 2.6 shows the point masses on the equivalent lengths at the various aspect rations.

Table 2.6: The point masses on the equivalent lengths of the flexible beam system at various aspect ratios

Point mass, m_i	L_o = 14.6625m Value (Kg) at β = 1.0	L_o = 14.9046m Value (Kg) at β = 1.25	L_o = 14.97034m Value (Kg) at β = 1.50	L_o = 14.98704m Value (Kg) at β = 1.75	L_o = 14.99433m Value (Kg) at β = 2.0
m_1	32228.9308	24267.0869	22665.0400	22178.1548	21988.7479
m_2	21850.9769	20438.9723	19932.6453	19764.4625	19710.5122
m_3	12143.4124	15505.4520	16085.9388	16255.6797	16329.1954
m_4	10643.4173	13937.4693	14828.8422	15102.4298	15207.2432
m_5	13226.1656	15494.9044	16085.7689	16251.3207	16328.9423
m_6	22136.8369	20439.2089	19938.3123	19763.9866	19705.7067
m_7	30881.7894	24269.3640	22666.1877	22178.3542	21990.5343

2.3.4 The Canonical Equations of Motion

The canonical equations of motions required to determine the vibration frequencies are as given in Eqn. (2.35).

$$\left(\delta_{11}m_1 - \frac{1}{\omega^2}\right)y_1 + \delta_{12}m_2y_2 + \delta_{13}m_3y_3 + \cdots + \delta_{17}m_7y_7 = 0$$
$$\delta_{21}m_1y_1 + \left(\delta_{22}m_2 - \frac{1}{\omega^2}\right)y_2 + \delta_{23}m_3y_3 + \cdots + \delta_{27}m_7y_7 = 0$$
$$\delta_{31}m_1y_1 + \delta_{32}m_2y_2 + \left(\delta_{33}m_3 - \frac{1}{\omega^2}\right)y_3 + \cdots + \delta_{37}m_7y_7 = 0$$
$$\vdots \quad (2.35)$$
$$\delta_{71}m_1y_1 + \delta_{72}m_2y_2 + \delta_{73}m_3y_3 + \cdots + \left(\delta_{77}m_7 - \frac{1}{\omega^2}\right)y_7 = 0$$

Where δ_{ij} is displacement, m_i is the point mass, ω is the cyclic frequency and y_i is the amplitude of vibration.

2.3.5 Numerical Experiment

In this paper, the parameters used for numerical experiment are: $E = 10.92MPa$, $\mu = 0.3$, L = 15m, b = 0.25m, h = open, and $\beta = {}^{h}/_{b}$.

Thus for non-zero amplitude of vibration, then the determinant of the coefficient of y_i must be zero. Table 2.7 presents numerical values of the displacements δ_{ij} for the various aspect ratios, β_i, using the defined parameters.

Table 2.7: The numerical values of displacements δ_{ij} at various aspect ratios

δ_{ij}	$\beta = 1.0$	$\beta = 1.25$	$\beta = 1.50$	$\beta = 1.75$	$\beta = 2.0$
δ_{11}	0.004434	0.002383	0.001398	0.000884	0.000592
$\delta_{12} = \delta_{21}$	0.007237	0.003806	0.002233	0.001411	0.000946
$\delta_{13} = \delta_{31}$	0.007851	0.004435	0.002476	0.001565	0.001049
$\delta_{14} = \delta_{41}$	0.007703	0.004142	0.002429	0.001535	0.001030
$\delta_{15} = \delta_{51}$	0.006923	0.003722	0.002183	0.001380	0.000925
$\delta_{16} = \delta_{61}$	0.005418	0.002913	0.001709	0.001080	0.000724
$\delta_{17} = \delta_{71}$	0.002894	0.001556	0.000912	0.000577	0.000387
δ_{22}	0.013037	0.006620	0.003882	0.002454	0.001646
$\delta_{23} = \delta_{32}$	0.014633	0.007605	0.004461	0.002820	0.001891
$\delta_{24} = \delta_{42}$	0.014632	0.007588	0.004450	0.002813	0.001885
$\delta_{25} = \delta_{52}$	0.013302	0.006889	0.004040	0.002553	0.001712
$\delta_{26} = \delta_{62}$	0.010495	0.005429	0.003184	0.002013	0.001350
$\delta_{27} = \delta_{72}$	0.007629	0.002913	0.001708	0.001080	0.000724
δ_{33}	0.017026	0.009157	0.005369	0.003393	0.002276

Table 2.7: The numerical values of displacements δ_{ij} at various aspect ratios, cont'd

δ_{ij}	$\beta = 1.0$	$\beta = 1.25$	$\beta = 1.50$	$\beta = 1.75$	$\beta = 2.0$
$\delta_{34} = \delta_{43}$	0.017440	0.009379	0.005500	0.003475	0.002325
$\delta_{35} = \delta_{53}$	0.016080	0.008649	0.005071	0.003204	0.002150
$\delta_{36} = \delta_{63}$	0.012810	0.006889	0.004040	0.002553	0.001713
$\delta_{37} = \delta_{73}$	0.006922	0.003723	0.002183	0.001380	0.000925
δ_{44}	0.018475	0.009935	0.005826	0.003681	0.002470
$\delta_{45} = \delta_{54}$	0.017439	0.009380	0.005500	0.003475	0.002331
$\delta_{46} = \delta_{64}$	0.014112	0.007590	0.004450	0.002813	0.001887
$\delta_{47} = \delta_{74}$	0.007702	0.004143	0.002429	0.001535	0.001030
δ_{55}	0.017025	0.009157	0.005369	0.003393	0.002276
$\delta_{56} = \delta_{65}$	0.014148	0.007609	0.004461	0.002820	0.001891
$\delta_{57} = \delta_{75}$	0.007848	0.004222	0.002475	0.001565	0.001049
δ_{66}	0.012312	0.006621	0.003883	0.002455	0.001646
$\delta_{67} = \delta_{76}$	0.007079	0.003808	0.002232	0.001411	0.000946
δ_{77}	0.004432	0.002384	0.001397	0.000884	0.000593

2.3.6 Evaluation of Vibration Frequencies

Equation (2.35) can be represented in matrix form as shown in Eqn. (2.36).

$$\begin{bmatrix} (\delta_{11}m_1 - R)\ \delta_{12}m_2\ \delta_{13}m_3\ \delta_{14}m_4\ \delta_{15}m_5\ \delta_{16}m_6\ \delta_{17}m_7 \\ \delta_{21}m_1\ (\delta_{22}m_2 - R)\ \delta_{23}m_3\ \delta_{24}m_4\ \delta_{25}m_5\ \delta_{26}m_6\ \delta_{27}m_7 \\ \delta_{31}m_1\ \delta_{32}m_2\ (\delta_{33}m_3 - R)\ \delta_{34}m_4\ \delta_{35}m_5\ \delta_{36}m_6\ \delta_{37}m_7 \\ \delta_{41}m_1\ \delta_{42}m_2\ \delta_{43}m_3\ (\delta_{44}m_4 - R)\ \delta_{45}m_5\ \delta_{46}m_6\ \delta_{47}m_7 \\ \delta_{51}m_1\ \delta_{52}m_2\ \delta_{53}m_3\ \delta_{54}m_4\ (\delta_{55}m_5 - R)\ \delta_{56}m_6\ \delta_{57}m_7 \\ \delta_{61}m_1\ \delta_{62}m_2\ \delta_{63}m_3\ \delta_{64}m_4\ \delta_{65}m_5\ (\delta_{66}m_6 - R)\ \delta_{67}m_7 \\ \delta_{71}m_1\ \delta_{72}m_2\ \delta_{73}m_3\ \delta_{74}m_4\ \delta_{75}m_5\ \delta_{76}m_6\ (\delta_{77}m_7 - R) \end{bmatrix} \begin{bmatrix} y_1 \\ y_2 \\ y_3 \\ y_4 \\ y_5 \\ y_6 \\ y_7 \end{bmatrix} = \begin{bmatrix} 0 \\ 0 \\ 0 \\ 0 \\ 0 \\ 0 \\ 0 \end{bmatrix} \quad (2.36)$$

Where $R = \frac{1}{\omega^2}$ (2.37)

Equation (2.36) is a homogeneous equation, and for non-zero values of the amplitudes y_i, the nontrivial solution is obtained by setting the determinant of the coefficient matrix of the amplitudes, y_i equal to zero, as expressed in Eqn. (2.38).

$$\begin{vmatrix} (\delta_{11}m_1 - R)\ \delta_{12}m_2\ \delta_{13}m_3\ \delta_{14}m_4\ \delta_{15}m_5\ \delta_{16}m_6\ \delta_{17}m_7 \\ \delta_{21}m_1\ (\delta_{22}m_2 - R)\ \delta_{23}m_3\ \delta_{24}m_4\ \delta_{25}m_5\ \delta_{26}m_6\ \delta_{27}m_7 \\ \delta_{31}m_1\ \delta_{32}m_2\ (\delta_{33}m_3 - R)\ \delta_{34}m_4\ \delta_{35}m_5\ \delta_{36}m_6\ \delta_{37}m_7 \\ \delta_{41}m_1\ \delta_{42}m_2\ \delta_{43}m_3\ (\delta_{44}m_4 - R)\ \delta_{45}m_5\ \delta_{46}m_6\ \delta_{47}m_7 \\ \delta_{51}m_1\ \delta_{52}m_2\ \delta_{53}m_3\ \delta_{54}m_4\ (\delta_{55}m_5 - R)\ \delta_{56}m_6\ \delta_{57}m_7 \\ \delta_{61}m_1\ \delta_{62}m_2\ \delta_{63}m_3\ \delta_{64}m_4\ \delta_{65}m_5\ (\delta_{66}m_6 - R)\ \delta_{67}m_7 \\ \delta_{71}m_1\ \delta_{72}m_2\ \delta_{73}m_3\ \delta_{74}m_4\ \delta_{75}m_5\ \delta_{76}m_6\ (\delta_{77}m_7 - R) \end{vmatrix} = 0 \quad (2.38)$$

Thus for a given aspect ratio $\beta_{i,}$ and by substituting appropriately the numerical values of point masses m_i and the numerical values of the displacements δ_{ij} from Tables 2.6 and 2.7 respectively into Eqn. (2.38), the eigenvalues obtained by solving Eqn. (2.38) yield the vibration frequencies. Thus from Tables 2.6 and 2.7, and at aspect ratio, $\beta = 1$, then Eqn. (2.38) reduces to Eqn. (2.39).

$$\begin{vmatrix} 142.90308 - R & 158.13552 & 95.33793 & 81.98624 & 91.56474 & 119.93738 & 89.37190 \\ 233.24077 & 284.87119 - R & 177.69455 & 155.73448 & 175.93445 & 232.32610 & 235.59717 \\ 253.02934 & 319.74534 & 206.75374 - R & 185.62120 & 212.67674 & 283.57288 & 213.76375 \\ 248.25945 & 319.72349 & 211.78111 & 196.63713 - R & 230.65110 & 312.39504 & 237.85154 \\ 223.12089 & 290.66169 & 195.26607 & 185.61055 & 225.17547 - R & 313.19197 & 242.36028 \\ 174.61635 & 229.32600 & 155.55711 & 150.19990 & 187.12379 & 272.54874 - R & 218.61219 \\ 93.27053 & 166.70110 & 84.05670 & 81.97560 & 103.79895 & 156.70667 & 136.86809 - R \end{vmatrix} = 0 \quad (2.39)$$

The solution of the characteristic equation of Eqn. (2.39) in terms of R and subsequently in terms of ω, gives the natural frequencies of vibration of simply supported rectangular flexible beam at aspect ratio equal to one. Therefore by carrying out similar procedure as per described above with respect to each aspect ratio, the desired natural frequencies are obtained. Thus, Table 2.8 presents the numerical values of highly approximated natural frequencies of simply supported flexible rectangular isotropic beam carrying a uniformly distributed mass elements.

Table 2.8: Numerical values of natural frequencies of simply supported flexible isotropic rectangular beam carrying a uniformly distributed mass elements

Natural frequency, (rad/sec)					
Mode	Aspect ratio, β				
	$\beta = 1.00$	$\beta = 1.25$	$\beta = 1.50$	$\beta = 1.75$	$\beta = 2.00$
ω_1	0.1845i	0.9773i	2.7458	3.1916	2.9861
ω_2	1.4781	1.4824	1.6680	2.1289	2.5173
ω_3	0.6869	0.7169	1.1288	1.4144	1.6650
ω_4	0.2751	0.5834	0.7416	0.9327	1.1484
ω_5	0.1467	0.3377	0.4284	0.5402	0.6640
ω_6	0.1091	0.1421	0.1905	0.2409	0.2948
ω_7	0.0272	0.0366	0.0476	0.0597	0.0730

Appendix A1: A system of bending moment diagrams due to unit load applied at various mass points for β = 1.0

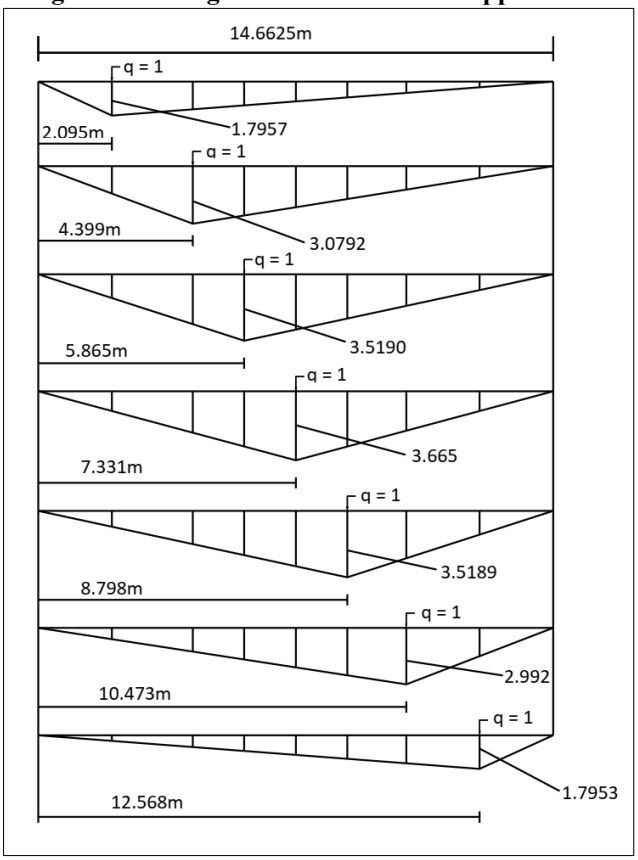

Appendix A2: A system of bending moment diagrams due to unit load applied at various mass points for β = 1.25

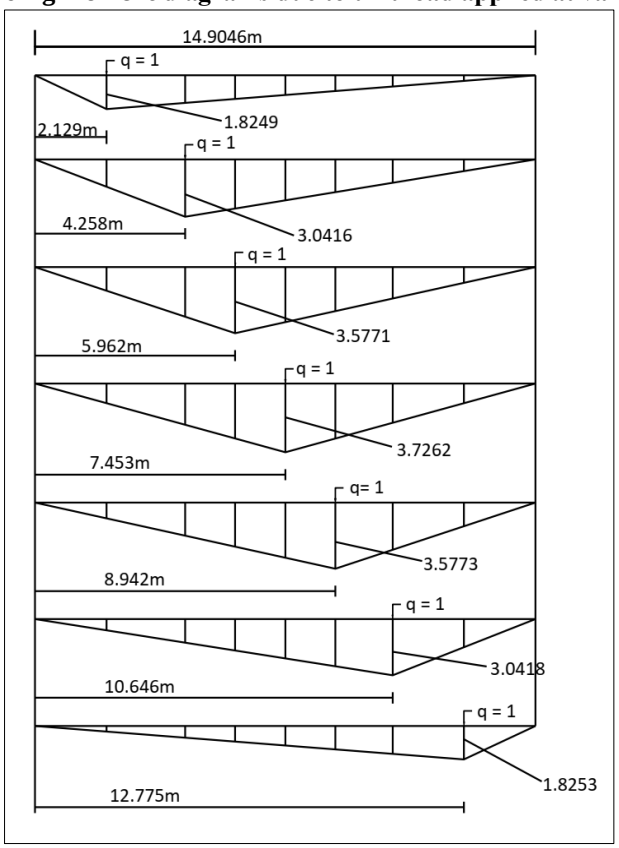

Appendix A3: A system of bending moment diagrams due to unit load applied at various mass points for β = 1.50

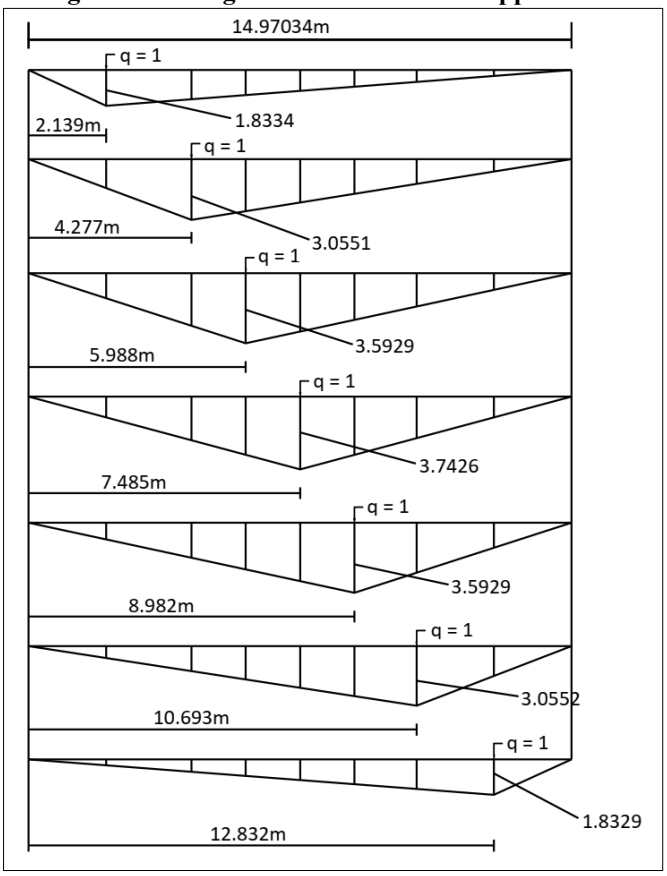

Appendix A4: A system of bending moment diagrams due to unit load applied at various mass points for β = 1.75

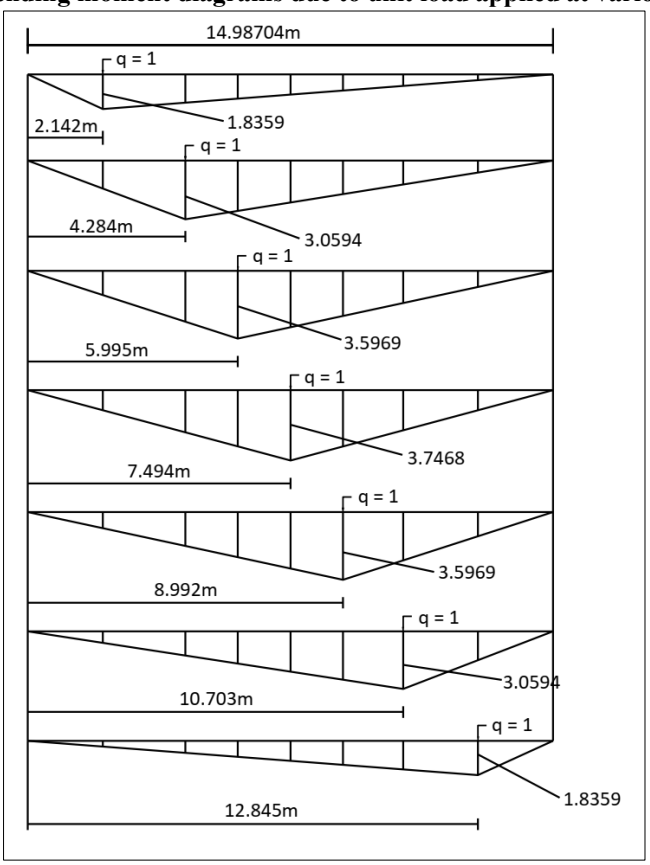

Appendix A5: A system of bending moment diagrams due to unit load applied at various mass points for β = 2.0

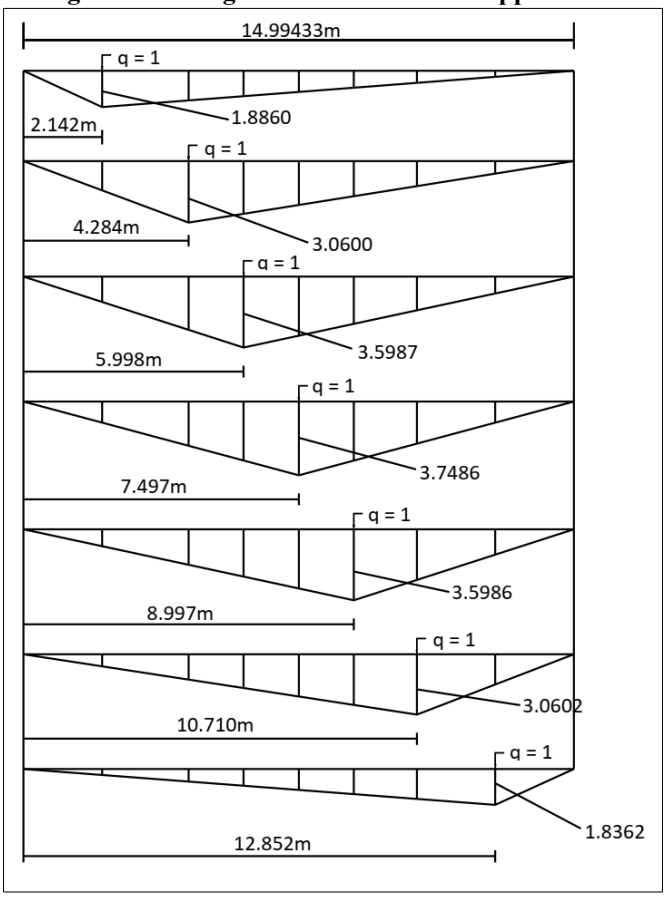

2.4 DISCUSSION OF RESULTS

From Tables 2.1 through 2.5, it was observed that at the mid-spans of the equivalent lengths, the elastic bending moments M_x and the nonlinear bending moments M_e' are numerically equal for all the aspect ratios. However, it was observed that the nonlinear bending moments exhibit linearly integer multiple of the elastic bending moments immediately after the end supports, which diminish towards the mid-spans of the equivalent lengths. For instance, at aspect ratio, β =1.0, the nonlinear bending moments are about 1.117 and 1.045 times the corresponding elastic bending moments at distances 2.095m and 4.395m measured from the end supports respectively. And at aspect ratio, β = 1.50, the nonlinear bending moments at distances 2.139m and 4.277m measured from the end supports are about 1.011 and 1.005 times the elastic bending moments respectively. Also at aspect ratio, β = 2.00, at distances 2.142m and 4.284m measured from the end supports, the nonlinear bending moments are about 1.002 and 1.001 times the elastic bending moments respectively. Furthermore, it was observed that the difference between nonlinear bending moments and elastic bending moments exhibits soft-spring type with aspect ratio, β. Equally, it was observed that the difference between the initial (undeformed) length, L and the corresponding equivalent length, L_o also exhibits soft-spring type with the aspect ratio, as the numerical values of Δ determined at aspect ratios β = 1.00, β = 1.50 and β = 2.00 are 0.3375m, 0.02966m and 0.00567m respectively for initial length of 15m. The implication of this disposition is that deepness of the beam influences the level of deformation of the beam.

From Table 2.8, it was observed that the first mode circular frequencies at aspect ratios, β = 1.00 and β = 1.25 are complex values. This exposition significantly shows that the beam at those aspect ratios experiences underdamped phenomenon; or in other words, the stability of the beam at those aspect ratios is not guaranteed for undeformed length of 15m. Also from Table 2.8, the fundamental frequency for each aspect ratios is located at the seventh mode; and the fundamental frequency exhibits hard-spring type with the aspect ratio. Also from Table 2.8, it was apparently observed that the natural frequencies decrease from mode number one to mode number seven; and the implication of this can be interpreted that the rigidity of the support influences the numerical value of the circular frequency, since mode number seven is close to the movable edge support.

CONCLUSIONS

This paper analyses vibration of uniform flexible simply supported rectangular isotropic beam under large deformation with uniformly distributed mass

elements using the equivalent pseudolinear system. In the analysis, it was found that the computed elastic bending moments and the large deformation (nonlinear) bending moments are numerically equal at the mid-spans of the equivalent lengths for all the aspect ratios. Also it was found that the difference between nonlinear bending moments and elastic bending moments exhibits soft-spring type with aspect ratio, β. Furthermore, it was found that the first mode circular frequencies at aspect ratios $\beta = 1.00$ and $\beta = 1.25$ are complex eigenvalues. Also, it was found that the natural frequencies exhibit hard-spring type with the aspect ratios, except at the first mode of aspect ratio $\beta = 1.75$. Furthermore, it was found that the fundamental frequency of each of the aspect ratios is located at the seventh mode. Therefore from these results obtained the following conclusions can be deduced:

(i) Maximum large deformation bending moment for a simply supported flexible rectangular isotropic beam loaded with uniformly distributed loads can be determined by using elastic model whenever the appropriate linearly horizontal displacement of the movable edge support is included in the expression of the bending moment.

(ii) Deepness of the flexible simply supported rectangular beam influences the magnitude of deformation under uniformly distributed loads.

(iii) The dynamic stability of flexible simply supported rectangular beam is not guaranteed when the depth-to-breadth ratio is less than or equal to 1.25.

(iv) The vibration characteristics of simply supported rectangular flexible beam loaded with uniformly distributed mass elements are influenced by the rigidity of the support conditions.

Conflict of Interest

The authors are hereby stated that there are no potential conflicts of interest with respect to the authorship and publication of this paper.

Funding

The authors of this paper received no financial support from any individual or organization for the research, authorship and publication of this paper

REFERENCES

- Awrejcewicz, J., Krysko, A. V., Soldatov, V., & Krysko, V. A. (2012). Analysis of the nonlinear dynamics of the Timoshenko flexible beams using wavelets.
- Chen, Q., & Levy, C. (1999). Vibration analysis and control of flexible beam by using smart damping structures. *Composites Part B: Engineering*, *30*(4), 395-406.
- Darkov, A. (1983). Structural mechanics, 4th edition. Moscow. MIR Publishers.
- Fan, W., & Zhu, W. D. (2016). An Accurate Singularity-Free Formulation of a Three-Dimensional Curved Euler-Bernoulli Beam for Flexible Multibody Dynamic Analysis. Proceedings of the ASME 2016 International Design Engineering Technical Conferences and Computers and Information in Engineering Conference, August 21 – 24, Charlotte, North Carolina, 1 – 9.
- Fertis, D. G. (1999). Nonlinear Mechanics, 2nd edition. Florida. CRC Press LLC.
- Fertis, D. G., & Afonta, A. (1992). Free vibration of variable stiffness flexible bars. *Computers & structures*, *43*(3), 445-450.
- Fertis, D. G., & Afonta, A. O. (1993). Small Vibrations of Flexible Bars by Using the Finite Element Method with Equivalent Uniform Stiffness and Mass Methodology. *Journal of Sound and Vibration*, *163*(2), 343 – 358.
- Fertis, D. G., & Lee, C. T. (1991). Inelastic analysis of flexible bars using simplified nonlinear equivalent systems. *Computers & structures*, *41*(5), 947-958.
- Fertis, D. G., & Schubert, F. R. (1994). Inelastic analysis of prismatic and nonprismatic aluminum members. *Computers & structures*, *52*(2), 287-295.
- Fertis, D. G., Taneja, R., & Lee, C. T. (1991). Equivalent systems for inelastic analysis of non-prismatic members. *Computers & structures*, *38*(1), 31-39.
- Gafsi, W., Najar, F., Choura, S., & El-Borgi, S. (2014). Confinement of vibrations in variable-geometry nonlinear flexible beam. *Shock and Vibration*, *2014*.
- Guo, X., Yang, X., Liu, F., Liu, Z., & Tang, X. (2020). Dynamic analysis of the flexible hub-beam system based on rigid-flexible coupling mechanism. *Proceedings of the Institution of Mechanical Engineers, Part K: Journal of Multi-body Dynamics*, *234*(3), 536-545.
- He, W., & Liu, J. (2019). Active Vibration Control and Stability Analysis of Flexible Beam Systems. Beijing China. Tsinghua University Press.
- Kwak, M. K. (1998). New Admissible Functions for the Dynamic Analysis of a Slewing Flexible Beam. *Journal of Sound and Vibration*, *210*(5), 581 – 592.
- Li, J., Liu, C. S., Li, F., & Wang, Z. X. (2012). Modal analysis of a flexible beam attaching multiple absorbers. *Applied Mechanics and Materials*, *226*, 154-157.
- Nayfeh, A. H., Emam, S. A., Preidikman, S., & Mook, D. T. (2003). An exact solution for the natural frequencies of flexible beams undergoing overall motions. *Journal of Vibration and Control*, *9*(11), 1221-1229.
- Pai, P. F., & Palazotto, A. (1996). Large-deformation analysis of flexible beams. *International Journal of Solids and Structures*, *33*(9), 1335-1353.

- Shvartsman, B. S. (2009). Direct method for analysis of flexible cantilever beam subjected to two follower forces. *International Journal of Non-Linear Mechanics*, *44*(2), 249-252.
- Trivedi, M. V., Banavar, R. N., & Kotyczka, P. (2016). Hamiltonian modelling and buckling analysis of a nonlinear flexible beam with actuation at the bottom. *Mathematical and Computer Modelling of Dynamical Systems*, *22*(5), 475-492.
- WEEKS, G. E., & JACKSON, J. E. (1971). Vibration characteristics of flexible beams about nonlinear equilibrium states. *AIAA Journal*, *9*(10), 2081-2083.
- Zhang, J., Rui, X., Liu, F., Zhou, Q., & Gu, L. (2017). Substructuring technique for dynamics analysis of flexible beams with large deformation. *Journal of Shanghai Jiaotong University (Science)*, *22*, 562-569.
- Zhang, W. X., & Yang, L. M. (2020). Study on Vibration of Flexible Beams with Interior Fluid. IOP Conf. Series: *Earth and Environmental Science 525*, 1 – 4.